RESEARCH

Performance Analysis of Plasmonic Nano-antenna Based on Graphene with Different Dielectric Substrate Materials for Optoelectronics Application

Saman Khabbat Ezzulddin[1] · Sattar Othman Hasan[2] · Mudhaffer Mustafa Ameen[3]

Abstract

The graphene-based plasmonic antenna's operating frequency and performance are significantly controlled by the substrate dielectric material. In this article, a plasmonic microstrip antenna is designed and simulated for terahertz applications. The design procedure is performed by testing different dielectric substrate materials of the same thickness, such as RT5800, polyimide, quartz, silicon dioxide (SiO_2), FR4, mica, silicon nitride (SiO_3N_4), and gallium arsenide (GaAs). Generally, the computed results reveal that the quartz substrate maintains suitable radiation performance with a minimum S11 values of -45.67 dB, efficiency of 92.65%, gain of about 3.15 dB, and bandwidth values of 310 GHz. Furthermore, a modification is done in the antenna by increasing the substrate height to obtain tri-band radiation mode. The results indicate that the proposed antenna operates at tri-band frequencies when the substrate thickness is larger than 6 μm. However, a better antenna radiation performance is observed with a substrate thickness of 7 μm which operates at frequencies of 0.766, 3.285, and 4.510 THz. Additionally, the overall radiation performance obtained for the proposed antennas of a single band frequency with quartz and dual and triple band frequencies with GaAs is compared with previous study results done by other researchers and a reliable agreement with an advancement in present work, especially in terms of antenna size and bandwidth. Finally, it can be said that the implementation of a graphene patch conductor to develop milt-band resonance frequency is an easy technique with low profiles, simple and alternative to the implementing conducting material slots, or extensions along the patch radiating borders techniques.

Keywords Graphene material · Nano-antenna · Microstrip antenna · Optoelectronic application

Introduction

In recent years, one of the significant concerns for modern photonic and electronic devices is closing to the terahertz (THz) gap which is located between the highest frequencies of photonics and the lowest frequencies of electronics. Furthermore, the equipment which generated and detected the electromagnetic (EM) radiation in that region is called an optoelectronics device [1].

Nowadays, the optoelectronics research field has become so interested in plasmonic nano-antennas, which radiate in multiple band frequencies. The experts continuously work to create a novel plasmonic antenna that successfully connects the free space radiation and concentrated subwavelength energy of restricted electromagnetic (EM) radiation [2]. Plasmonic antennas are being widely implemented in a number of new applications, including sensing, spectroscopy, nonlinear optics, nanophotonic circuitry, optical metasurfaces, photodetection, and better photoemission [3].

The terahertz range from (0.1 to 10) THz, and it is placed between the infrared (IR) and millimeter (mm) wave. It is provides wide bandwidths in the hundreds of gigahertz range, extremely high data rate, and smaller attenuation than optical signals [4–6]. Nevertheless, in this frequency band, conventional metallic conductors

✉ Saman Khabbat Ezzulddin
saman.ezzlddin@su.edu.krd

1 Department of Physics, College of Science, Salahaddin University, Erbil, Iraq

2 Department of Physics, College of Education, Salahaddin University, Erbil, Iraq

3 Department of Physics, College of Education, Tishk International University, Erbil, Iraq

are unable to be appropriate as a result of the presence of low conductivity and high skin effect, which causes a high loss in the antenna radiation performances, due to low electron mobility in the metallic structure at the THz frequency band [7, 8]. However, the low skin effect, permanent tunability through the electrostatic gating, and chemical potential of graphene make it a good alternative conductor material, which is mostly interesting for designing and fabricating antenna in THz applications [9]. Graphene is widely employed in many different kinds of industry sectors, including photonics, telecommunications, and electronics [10]. Moreover, it plays an important role for the development of planar adaptable antennas having multi-functional manners for determining the state of electromagnetic (EM) waves in terms of polarization, operating frequency, and antenna radiation patterns [11–13].

Therefore, these properties of graphene encouraged researchers to develop many different types of graphene-based antennas having currently observed performance in the terahertz range. For instance, in [14], a Vivaldi antenna is developed using graphene layers to improve the antenna bandwidth as the Fermi energy level is increased. In [15], the graphene material capability was implemented to design microstrip antennas of square patch shapes to regulate and control antenna polarization. Moreover, a tunable graphene antenna which consist of a radiating graphene patch and a non-radiating graphene ring was suggested and investigated in transverse magnetic (TM22) mode by [16]. Additionally, the effect of size and repetition of the photonic crystal on the antenna radiation characteristics in the THz frequency bands was also studied by [17]. Furthermore, a number of multi-beam tunable graphene-based dipole antennas incorporating reflector-transmission and reflector-director windows techniques for modulation were investigated in the THz band. On the other hand, in [18–20], a different microstrip antenna–based graphene having polarization variance was proposed by changing the chemical potential of the graphene patch to achieve linear polarization, right-hand circular polarization (RHCP), and left-hand circular polarization (LHCP) in the antennas far-field radiation pattern.

In this article, plasmonic microstrip antennas based on graphene with different dielectric substrates are designed and simulated to operate in the frequency band ranges from 0.1 to 5 THz. In addition, the dielectric substrate thickness is also modified to allow the antenna to operate at multi-band frequency operations. The simulation procedure was performed by implementing a full-wave electromagnetic model based on the finite integration technique (FIT) technique. The remaining part of the present work is organized as follows. In the "Material Method" section, the graphene properties and configuration of the plasmonic microstrip antenna are described. Outcomes of the proposed antenna simulation

are mentioned in "Results and Discussion" section. Afterward, the "Conclusion" section shows the conclusions.

Material Method

The proposed plasmonic microstrip antenna based on graphene is designed, simulated, and optimized using an electromagnetic (EM) simulator named computer simulation technology (CST), which is based on a finite integration technique (FIT) [21]. In its simple construction, the microstrip antenna is composed of a dielectric substrate sandwiched between two conductor materials as illustrated in Fig. 1.

In this figure, the substrate thickness is denoted by h, while the width and length of patch and ground plane conductor material dimensions are represented by $\underline{L}_p$, L_g, W_p, and W_g, respectively. The characteristic and properties of graphene material and its construction are explained in the following sub-section.

Properties of Graphene

Graphene is a new nanomaterial made of a very thin two-dimensional (2D) carbon atom layer within a hexagonal honeycomb lattice. It is a unique material in which the relationship between the energy and momentum of electrons is linear instead of quadratic during a variety of energies [22]. This behavior led to the creation of very high carrier mobility at room temperature. Also, this extraordinary characteristic of graphene allows it to be extremely attractive for supporting and promoting surface plasma polaritons (SPPs)' mode, particularly in the range of terahertz (THz) band, where its resonance plasma frequency is perfectly placed in this spectrum [23].
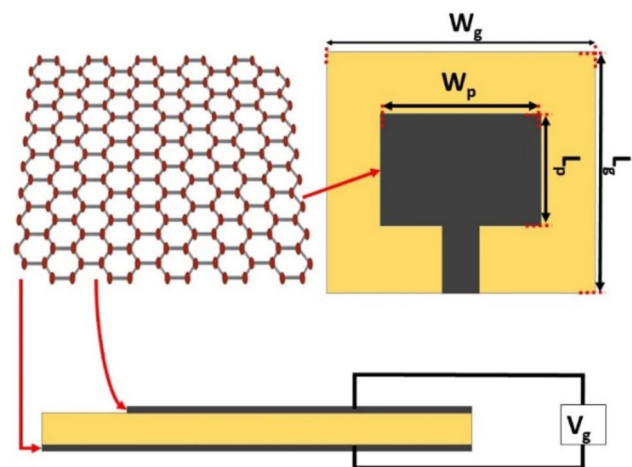
Fig. 1 Schematic diagram shows the designed graphene microstrip antenna

Furthermore, the surface conductivity of graphene (σ_s) is dependent on the frequency that can be determined by its values approximately using Kubo's equation, which consists of two parts, interband conductivity and intraband conductivity, as given by [24]:

$$\sigma_s(\omega, \mu_c) = \sigma_{intra}(\omega, \mu_c) + \sigma_{inter}(\omega, \mu_c) \tag{1}$$

The graphene intraband conductivity (σ_{intra}) term can be represented as [25]:

$$\sigma_{intra}(\omega, \mu_c) = -j\frac{2e^2 K_B T}{\pi \hbar^2}\ln\left(2\cosh\left(\frac{\varphi_c}{2}\right)\right)\cdot\frac{1}{\omega - j\tau^{-1}} \tag{2}$$

The graphene interband conductivity (σ_{inter}) term can be represented as [25]:

$$\sigma_{inter}(\omega, \mu_c) = \frac{e^2}{4\hbar}\left(H\left(\frac{\omega}{2}\right) + j\frac{4\omega}{\pi}\int_0^\infty \frac{H(\varepsilon) - H\left(\frac{\omega}{2}\right)}{\omega^2 - 4\varepsilon^2}d\varepsilon\right) \tag{3}$$

where $H(\varepsilon) = \frac{\sinh\varphi}{\cosh\varphi_c + \cosh\varphi}$, $\varphi_c = \frac{\mu_c}{K_B T}$ and $\varphi = \frac{\hbar\varepsilon}{K_B T}$

where μ_c is the chemical potential, T is temperature, K_B is a Boltzmann's constant, ω is the angular frequency, $\hbar$ = reduced Planck's constant, τ is relaxation time, and e is the charge of the electron. In this article, the value of μ_c is assumed to be equal to 0.1 eV, $K_B = 8.62$ eVK^{-1}, $T = 300$ K, $\tau = 1$ ps, $\hbar = 6.582 \times 10^{-16}$ eVs, and e $= 1.6 \times 10^{-19}$ C. According to the Pauli exclusion principle, the intraband surface conductivity leads the total value of surface conductivity (σ_s) at low frequency in the range of THz. Meanwhile the interband component experiences no influence on the overall surface conductivity (σ_s) and, therefore, can be neglected [26].

Antenna Configuration

The proposed antenna was constructed from a single rectangular patch of graphene is putted at the upper part of the dielectric substrate. The opposing side of the substrate comprises a graphene layer of identical dimensions to the substrate that is used to create the antenna ground plane. The height of the ground plane and radiating patch is assumed to be equal to (0.34 nm). As the graphene patch is excited using electromagnetic waves (EM), the electrons inside it are moving back and forth at (THz) frequencies, and this phenomenon is referred to as surface plasma polariton (SPP) [27, 28]. The dispersion relation of possible maintained (TM) mode of plasmons or the SPP wavenumber (k_{SPP}) of the graphene layer is expressed in free space as [29]:

$$k_{SPP} = k_\circ\sqrt{1 - \left(\frac{2}{\eta_{eff}\sigma_g}\right)^2} \approx \frac{\hbar\omega^2}{2\alpha\mu_c c} \tag{4}$$

$$\eta_{eff} = \sqrt{1 - \frac{4\mu_\circ}{\varepsilon_\circ(\sigma_g)^2}} \approx \frac{\lambda}{\lambda_{SPP}} \tag{5}$$

where η_{eff} and k_0 are effective intrinsic impedance of free space and wavenumber of graphene material, respectively. Furthermore, the effective intrinsic impedance of graphene sheet is associated with both the free space permittivity (ε_0) and permeability (μ_0). The dimensions of a plasmonic microstrip antenna are determined from the equations presented by [30] as:

$$W_p = \frac{(2M + 1)}{\sqrt{\varepsilon_r}} \times \frac{\lambda_\circ}{2} \tag{6}$$

$$L_p = \frac{(2N + 1)}{\sqrt{\varepsilon_{eff}}} \times \left(\frac{\lambda_{spp}}{2}\right) - 2\Delta L \tag{7}$$

where N and M are positive integers (in this paper are regarded as, N = M = 1); λ_{spp} and λ_0 are the operating and free space wavelengths; ΔL is the patch length extension as a result of the fringing effect; and (ε_r) and (ε_{eff}) are relative dielectric constant and the effective dielectric constants, respectively. The width of the feeding line (W_f) is determined from the antenna total input impedance (Z_a) which can be obtained by:

$$Z_a = \frac{11.96\lambda_\circ}{W_f} \tag{8}$$

Furthermore, Z_a is matched in accordance with the accepted standard of 50 Ω impedance through the feeding line length (L_f) with the characteristic impedance, which is expressed as $Z_0 = 50 \times Z_a$. Consequently, the physical dimensions of the ground and substrate are determined using the equation that follows the expression:

$$W_s = W_g = W_p + 2L_f \tag{9}$$

$$L_s = L_g = L_p + 2L_f \tag{10}$$

where L_s is the length while W_s is the width of the dielectric substrate, respectively. The optimized dimensions of the proposed antennas are illustrated in Table 1.

Table 1 Optimized dimensions of the proposed microstrip antenna dimensions

Parameter	W_p	W_g	W_f	L_p	L_g	L_f	h
Values in μm	40	70	8.763	30	60	15	4

Table 2 Electric, thermal, and mechanical characteristics of various substrate materials

Properties of substrate	Electrical properties		Thermal properties			Mechanical properties	
	Dielectric constant	Loss tangent	Specific heat	Thermal conductivity	Coefficient of thermal expansion	Young's modulus	Density
Unit	-	-	J/kg.°K	W/K m	$10^{-6}/°C$	$N/m^2 \times 10^9$	(Kg/m^3)
RT5880	2.20	0.0009	960	0.2	1.10	-	1370
Polyimide	3.50	0.0027	1000	0.2	25.0	2.5	1400
Quartz	3.75	0.0004	700	5.0	8.0	7.5	2200
SiO_2	3.90	0.0010	680	1.5	4.5	6.6	2270
FR4	4.30	0.0250	1150	0.3	14.0	-	1850
Mica	6.00	0.0003	500	0.75	3.0	3.1	2800
SiO_3N_4	9.50	0.001	691	30	3.3	2.5	3290
GaAs	12.95	0.006	330	54	5.6	8.5	5320

Besides, selecting an appropriate dielectric substrate material plays an essential role to graphene antennas since the substrate's height (h) and dielectric constant (ε_r) significantly impact impedance characteristics and, therefore, the antenna operating frequency. Moreover, the substrate material can be attributed to changing charge carrier density in the graphene patch, which affects the carrier mobility numbers and supports graphene's tuned capabilities. Therefore, in this work, various substrate materials are chosen such as RT5800, polyimide, quartz, silicon dioxide (SiO_2), FR4, mica, silicon nitride (SiO_3N_4), and gallium arsenide (GaAs), each of which has its own thermal, electrical, and mechanical properties as summarized in Table 2.

The above-mentioned dielectric substrate materials are implemented for designing a plasmonic microstrip antenna operating at 1.0 THz using CST simulation techniques.

Results and Discussions

In the present work, radiation characteristics of the plasmonic microstrip antenna based on graphene are analyzed for various dielectric substrate materials using (CST) microwave studio simulation software at the resonate frequency of 1.0 THz. The performance of the recommended antenna is studied in terms of return loss (S11), voltage standing wave ratio (VSWR), impedance bandwidth (BW), efficiency, gain, and antenna radiation pattern such as E-plane and H-plane, and the results are presented and discussed in the form of graphs and tables in the following sub-sections.

Single and Dual Band Antenna

One of the most important antenna parameters is return loss (S11), and it should be less than -10 dB for appropriate impedance matching. Figure 2 shows the return loss (S11) according to operating frequency near 1.0 THz, which is -15.903 dB

for RT5880 at 0.995 THz, -40.059 dB for polyimide at 1.010 THz, -45.674 dB for quartz at 1.00 THz, -40.283 and -37.508 dB for SiO_2 at 0.990 THz, and -36.045, -29.435, -22.199, and -21.144 dB for FR-4, mica, SiO_3N_4, and GaAs at 0.985, 0.935, 0.870, and 0.825 THz, respectively.

In addition, the voltage standing wave ratio (VSWR) is also another important factor that should be taken into account during assessment of an antenna performance. A lower value of VSWR indicates that the antenna is properly matched to the transmission line feed, and this means a greater amount of power that is transmitted to the antenna terminal. Besides, the antenna bandwidth, gain, and antenna efficiency for each dielectric substrate materials are computed, and the results are presented in Table 3.

This table says that each of the considered dielectric substrates maintains a reliable VSWR values near to unity and among which the quartz and SiO_2 provide lower S11 and VSWR values. Moreover, the antennas with both silicon
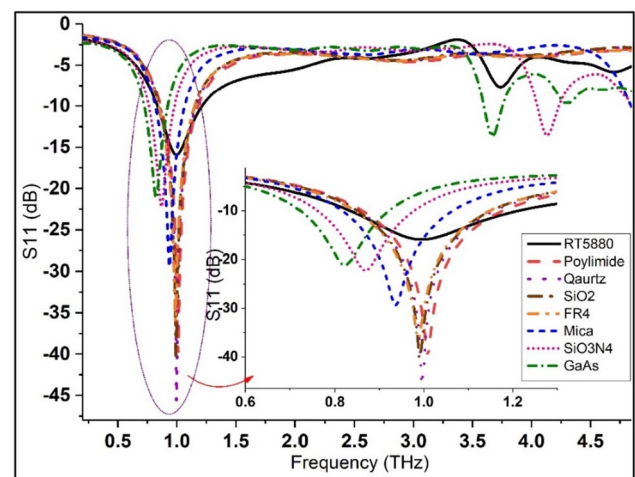
Fig. 2 Variation of S11 of proposed plasmonic antenna based on graphene with various substrates

Table 3 Performance comparison of proposed antenna for various substrate materials

Substrate	f_r (THz)	BW (THz)	FBW %	S11 (dB)	VSWR	Gain (dB)	Efficiency%
RT5880	0.995	0.382	38.492	-15.903	1.381	3.067	88.63
Polyimide	1.010	0.318	31.584	-40.059	1.020	3.122	93.41
Quartz	**1.000**	**0.310**	**31.200**	**-45.674**	**1.010**	**3.150**	**92.65**
SiO$_2$	0.990	0.302	30.606	-40.283	1.019	3.093	91.32
FR4	0.985	0.300	30.457	-36.045	1.032	3.091	86.73
Mica	0.935	0.250	26.738	-29.435	1.067	2.951	92.48
SiO$_3$N$_4$	0.870	0.199	24.121	-22.199	1.168	2.675	87.21
	4.134	0.162	4.328	-13.536	1.531	2.540	83.20
GaAs	0.825	0.218	25.172	-21.144	1.192	2.798	88.97
	3.674	0.178	4.436	-13.703	1.520	3.030	87.26

The bold entries indicates the reliable performance among other calculated results
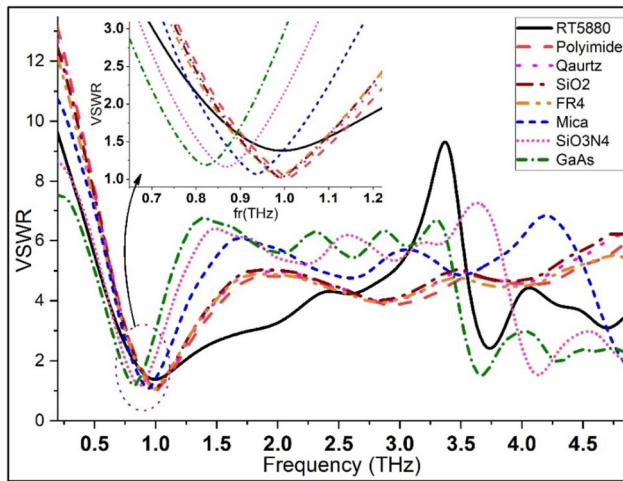
Fig. 3 Variation of VSWR of proposed plasmonic nano-antenna based on graphene with various substrates

nitrate and gallium arsenide substrate material are resonating at another band frequencies, which are 4.134 and 3.674 THz with S11 values of − 13.536 and − 13.703 dB and VSWR values of 1.531 and 1.520, respectively, as indicated in Figs. 2 and 3.

In addition, the 2-dimensional electric (E) and magnetic (H) plane radiation patterns for the first exaction mode (TM10) of the advised antenna with each assumed substrate materials are also calculated and the results are displayed in Fig. 4. It is clearly seen from these figures that the antennas' gain varies from 2.540 to 3.150 dB at their operating frequencies. The results also imply that the quartz substrate material provides peak values of antennas' gain and efficiency with acceptable antenna bandwidth. Consequently, the fundamental antenna parameters that are derived from the proposed antennas using RT5800, polyimide, quartz, SiO$_2$, FR4, mica, SiO$_3$N$_4$, and GaAs substrate materials, as
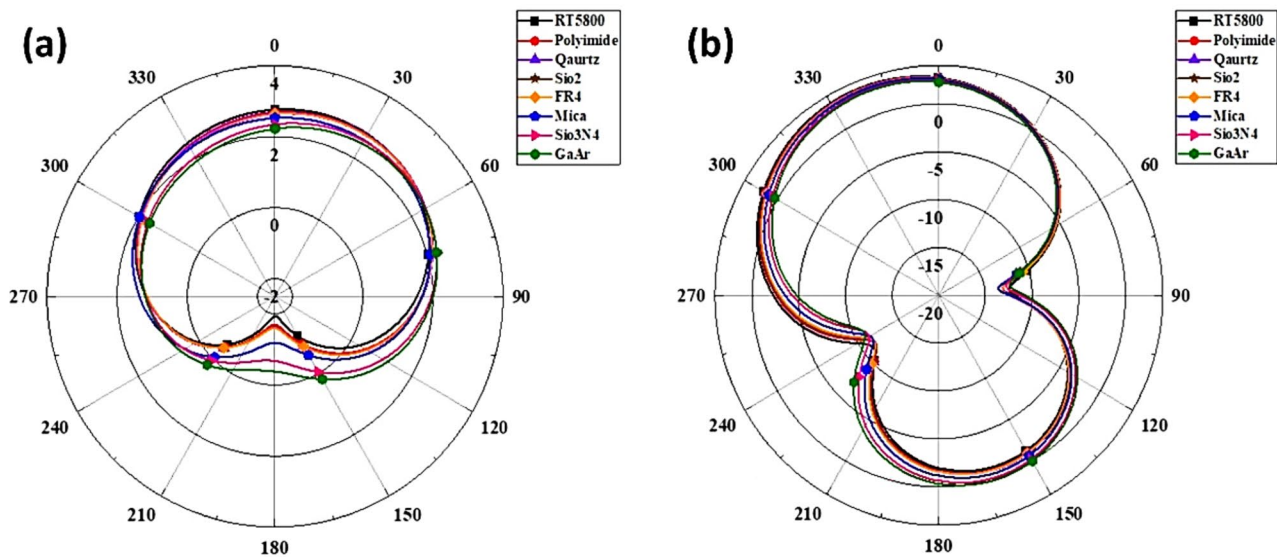
Fig. 4 2D view of the proposed antennas radiation pattern. **a** E-plane and **b** H-plane with different substrates for the first exaction mode (TM10)

Table 4 Antenna performance with the use of GaAs material of various substrate thickness

Substrate thickness (µm)	f_r (THz)	BW (THZ)	FBW%	S11 (dB)	VSWR	Gain (dB)	Efficiency%	Band
4	0.825	0.218	24.121	−21.144	1.192	2.798	88.97	Dual band
	3.674	0.178	4.436	−13.703	1.520	3.030	87.26	
5	0.810	0.201	25.419	−27.346	1.088	2.570	91.02	Dual band
	3.605	0.229	6.379	−17.973	1.289	3.370	87.90	
6	0.780	0.199	26.018	−41.066	1.017	2.540	84.67	Tri-band
	3.425	0.233	7.092	−23.330	1.146	2.760	80.76	
	4.720	0.310	6.878	−20.894	1.200	4.180	79.07	
7	0.766	0.203	26.384	−25.232	1.099	2.510	90.11	Tri-band
	3.285	0.224	3.903	−30.152	1.064	2.730	88.32	
	4.510	0.324	6.878	−30.852	1.059	6.560	85.56	
8	0.740	0.184	24.932	−21.698	1.179	2.780	82.81	Tri-band
	3.180	0.247	9.789	−31.498	1.054	2.830	76.54	
	4.340	0.284	6.601	−31.385	1.055	4.910	60.77	

presented in Table 3 can be regarded as a baseline comparison for identifying a suitable substrate for antenna designing in terahertz region.

Triple Band Antenna

In this section, the impact of substrate thicknesses on the antenna performances for GaAs substrate material is analyzed due to its wide usage in the solar cell applications and it also provides multi-band operation which makes it reliable for designing novel smart antennas operating at multi-operational frequencies. For this, the thickness of the GaAs substrates is varied from 4 to 8 µm, and the computation results for the antenna bandwidth, gain, and efficiency are demonstrated in Table 4. This table displays that the

proposed antenna is operated with a dual resonance frequency at 0.825 and 3.674 THz and 0.810 and 3.605 THz, respectively, for the substrate thickness 4 µm and 5 µm. Moreover, when the substrate thickness is raised to 6, 7, and 8 µm, a third resonance frequency occurs at 4.720, 4.510, and 4.340 THz, respectively. This behavior can be attributed to the creation of more fringing filed lines that arise at the edge of the dielectric substrates as the height of the substrate is increased. Therefore, the energy stored in the microstrip antenna resonator decreases. Hence, the quality (Q) factor drops, and hence, the bandwidth (BW) of the proposed antenna is improved.

Commonly, the graphene patch works exactly as a parallel plate transmission line, resonating between the feeding line and the ground plane. As a result, the basic vibration mode is TM10 [18]. Meanwhile, when the substrate
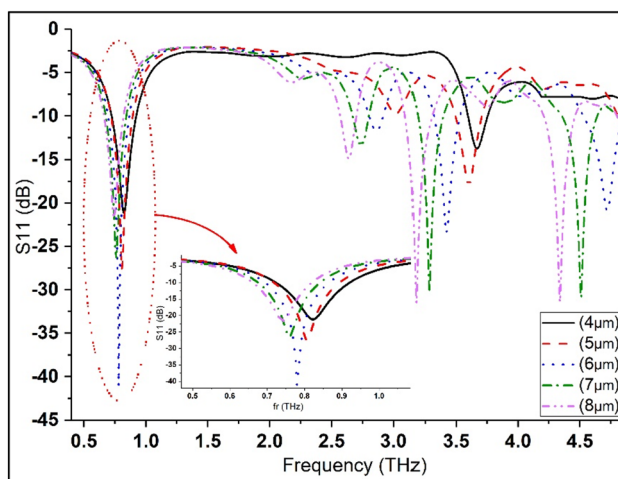
Fig. 5 Change of S11 as a function of frequency with various GaAs substrate thicknesses
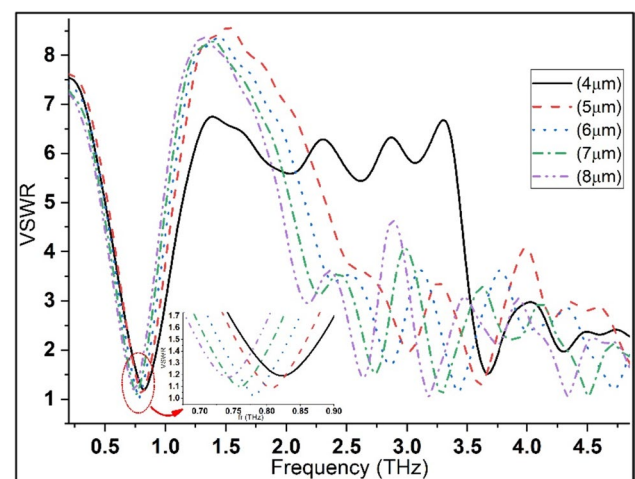
Fig. 6 Change of VSWR as a function of frequency with various GaAs substrate thicknesses
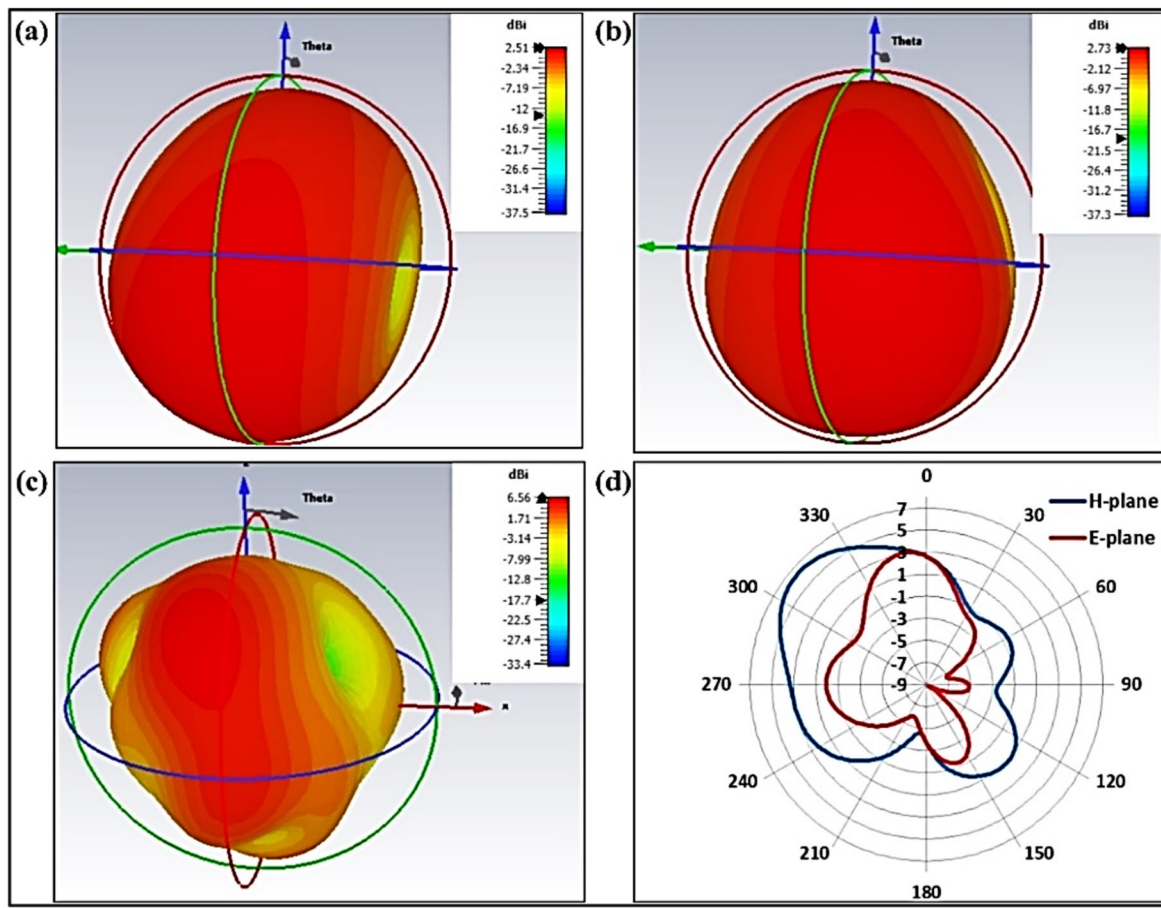
Fig. 7 3D radiation pattern at **a** 0.766 THz, **b** 3.285 THz, **c** 4.510 THz, and **d** E-plane and H-plane patterns at 4.510 THz (TM20) mode with the substrate thickness of 7 μm

thickness becomes thicker, enough space is formed inside the antenna substrate for a further higher-order vibration mode, such as TM11, TM20, and TM30 to propagate. The aforementioned mode will produce resonance equivalent to TM10 but with various frequencies because of a different phase constant. Therefore, the antenna substrate thickness can be adapted to provide triple-band operating frequencies. The optimum substrate thickness for triple-band resonance seems to occur at 7 μm and 8 μm. However, when the substrate thickness is raised to higher than this limitation, the capabilities of the antenna will be decreased with regard to surface wave propagation in the antenna resonator. In general, a proposed plasmonic microstrip graphene patch antenna is operated with a dual-band operating frequencies when the substrate thickness is of the order of 4 to 5 μm and beyond which it operates with triple-band frequencies as shown in Figs. 5 and 6.

Moreover, the 3D and 2D views of the far-field radiation pattern for the triple-band antenna for a GaAs substrate with a substrate thickness of 7 μm is calculated, and the results are displayed in Fig. 7. Additionally, the realized gains for

the plasmonic antenna with the optimized GaAs substrate thickness values of 7 μm is also calculated as a function of frequency, and the results are shown in Fig. 8. This figure
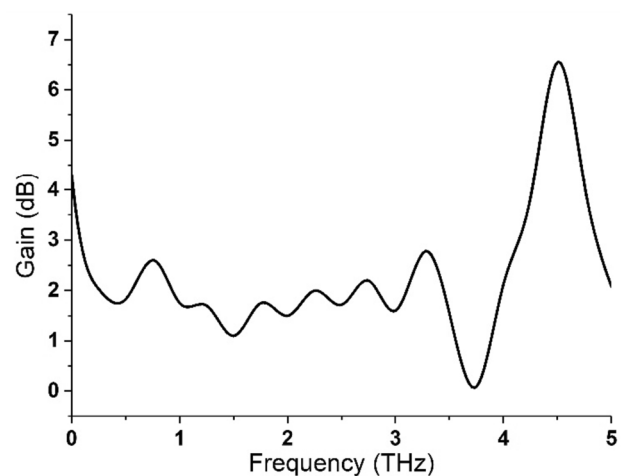
Fig. 8 Realized gain versus frequency of the proposed antenna built up on GaAs substrate with thicknesses of 7 μm

Table 5 Performance of the suggested antenna in comparison to state-of-the-art works

Band	Material	f_r (THz)	BW(GHz)	Gain (dB)	Dimensions (μm^3)	Reference
Single-band	Silicon	2.60	145.4	2.80	65×65×34	[31]
		0.34	30	7.9	200×200×530	[32]
	Arlon	0.72	270.0	-	120×120×45	[33]
		0.12	49	-	1500×1500×500	[34]
	SiO₂	0.95	125	2.45	93×120×25	[35]
		30	10.08	3.52	1800×1800×3.0	[36]
	Teflon	5.50	217.7	3.91	24×24×11.50	[37]
	Polyimide	0.11	9.4	-	1500×1500×500	[34]
		0.62,	34.9,	6.59	800×600×191	[30]
		0.63	36.23	7.93		
	RT/6006	0.74	97	10.0	1000×1000×200	[38]
	Duriode	0.13	49	-	1500×1500×500	[34]
	Quartz	**1.0**	**310**	**3.150**	**70×60×4.0**	**Present work**
Dual-band	FR4	3.50	400	1.46	120×95×10	[39]
		4.33	460	2.34		
	Teflon	4.33	199.6	2.76	24×24×11.50	[37]
		5.82	138.6	2.47		
	Silicon	2.48	115.1	2.70	65×65×34	[31]
		3.35	140.5	6.03		
	GaAs	**0.825**	**218**	**2.798**	**70×60×4.0**	**Present work**
		3.674	**178**	**3.030**		
Tri-Band	RT 5880	2.32	230	0.998	120×95×10	[39]
		3.53	520	1.930		
		4.38	610	2.58		
	SiO₂	1.95	-	4.79	50×50×30	[12]
		4.83	-	5.05		
		5.44	-	5.53		
	GaAs	**0.766**	**203**	**2.510**	**70×60×7.0**	**Present work**
		3.285	**224**	**2.730**		
		4.510	**324**	**6.560**		

The bold entries shows results in this work more clearly compared to the results of other previous works

again displays that our proposed antenna is operated at three band frequencies of 0.766, 3.285, and 4.51 THz with a gain value of 2.51, 2.73, and 6.56 dB, respectively.

Finally, the computed antenna gain, bandwidth, and antenna size of the present work at the single band (1 THz) for quartz substrate, dual-band (0.825 and 3.674) THz, and triple-band (0.766, 3.285, and 4.510) THz, frequency operation for GaAs substrate material, and those obtained by other researchers are summarized in Table 5. One clearly observes from this table that the size, gain, and bandwidth parameter values obtained for the proposed antennas are in a reliable agreement with those previously achieved by other research workers at single-, dual-, and triple-band operational frequencies. Additionally, our results are better than most of the available data presented in this table, especially regarding the antenna size and bandwidth values.

Conclusion

This work deals with the design of a plasmonic microstrip graphene patch antenna supporting dual- and tri-band resonance in the low THz frequency ranging from 0.1 to 5 THz. The analysis procedure is performed by implementing CST with the use of different dielectric substrate materials of the same thickness. The simulation result displays that the quartz substrate material maintains a minimum S11 value of − 45.674 dB with a suitable VSWR of 1.010 at the frequency of 1.0 THz with the gain, bandwidth, and efficiency values of 3.150 dB, 310 GHz, and 92.65%, respectively. In addition, the computed results also reveal that the GaAs and SiO_3N_4 operate at dual-band frequency with a reliable gain and bandwidth values.

Moreover, the simulation outcome indicates that, as the GaAs substrate thickness increased beyond 6 μm, the

proposed antenna operates with a tri-band operational frequency. However, a better value of gain of 2.510, 2.730, and 6.560 dB is attained for a 7-μm substrate thickness, corresponding to the frequencies of 0.766, 3.285, and 4.510 THz, respectively. On the other hand, this technique of using a graphene patch to develop milt-band resonance frequency can be regarded as an easy technique for modulation, low profiles, simple, and alternative to complexities compared to implementing conducting material slots, stacks, or extensions along the patch radiating borders techniques. Finally, the radiation performance of the proposed antenna seems to be better than most of the previously performed by other research workers, especially in terms of antenna size and bandwidth.

Declarations

References

1. Dhillon S et al (2017) The 2017 terahertz science and technology roadmap. J Phys D Appl Phys 50(4):043001
2. Moshiri SMM, Nozhat N (2021) Smart optical cross dipole nano-antenna with multibeam pattern. Sci Rep 11(1):5047. https://doi.org/10.1038/s41598-021-84495-0
3. Meng Y (2018) Ultracompact graphene-assisted tunable waveguide couplers with high directivity and mode selectivity. Sci Rep 8(1):13362. https://doi.org/10.1038/s41598-018-31555-7
4. Das P (2023) Beam-steering of THz MIMO antenna using graphene-based intelligent reflective surface. Opt Quantum Electron 55(8):711. https://doi.org/10.1007/s11082-023-04996-2
5. Fakharian MM (2022) A graphene-based multi-functional terahertz antenna. Optik 251:68431. https://doi.org/10.1016/j.ijleo.2021.168431
6. Nishtha RS, Yaduvanshi AK, Kushwaha Pandit AK (2021) Terahertz rectangular DRA for high speed communication applications. J Discrete Math Sci Cryptogr 24(5):1205–1214. https://doi.org/10.1080/09720529.2021.1932904
7. Khaleel SA, Hamad EKI, Saleh MB (2022) High-performance tri-band graphene plasmonic microstrip patch antenna using superstrate double-face metamaterial for THz communications. J Electr Eng 73(4):226–236, 3922. https://doi.org/10.2478/jee-2022-0031
8. Jamshed MA, Nauman A, Abbasi MAB, Kim SW (2020) Antenna selection and designing for THz applications: suitability and performance evaluation: a survey. IEEE Access 8:113246–113261. https://doi.org/10.1109/ACCESS.2020.3002989
9. Hanson GW (2008) Dyadic Green's functions for an anisotropic, non-local model of biased graphene. IEEE Trans Antennas Propag 56(3):747–757
10. Shamim SM, Trabelsi Y, Arafin N, Anushkannan NK, Dina US, Hossain MA, Islam N (2023) Design and analysis of microstrip patch antenna with photonic band gap (PBG) structure for high-speed THz application. Opt Quantum Electron 55(7):618. https://doi.org/10.1007/s11082-023-04834-5
11. Sharma SK, Chieh JCS (2021) Multifunctional antennas and arrays for wireless communication systems. John Wiley & Sons
12. Shalini M, Madhan MG (2020) Performance predictions of slotted graphene patch antenna for multi-band operation in terahertz regime. Optik 204:164223. https://doi.org/10.1016/j.ijleo.2020.164223
13. Lu G, Wang J, Xie Z, Yeow JTW (2022) Carbon-based THz microstrip antenna design: a review. IEEE Open J. Nanotechnol. 3:15–23. https://doi.org/10.1109/OJNANO.2021.3135478
14. Poorgholam-Khanjari S, Zarrabi FB (2021) Reconfigurable Vivaldi THz antenna based on graphene load as hyperbolic metamaterial for skin cancer spectroscopy. Optics Communications 480:126482. https://doi.org/10.1016/j.optcom.2020.126482
15. Kiani N, Hamedani FT, Rezaei P (2021) Polarization controlling plan in graphene-based reconfigurable microstrip patch antenna. Optik 244. https://doi.org/10.1016/j.ijleo.2021.167595
16. Varshney G (2020) Reconfigurable graphene antenna for THz applications: a mode conversion approach. Nanotechnol 31(13)
17. Khan MAK, Ullah MI, Alim MA (2021) High-gain and ultrawide-band graphene patch antenna with photonic crystal covering 96.48% of the terahertz band. Optik 227:166056. https://doi.org/10.1016/j.ijleo.2020.166056
18. Jafari Chashmi M, Rezaei P, Kiani N (2020) Polarization controlling of multi resonant graphene-based microstrip antenna. Plasmonics 15(2):417–426. https://doi.org/10.1007/s11468-019-01044-2
19. Jafari Chashmi M, Rezaei P, Kiani N (2020) Y-shaped graphene-based antenna with switchable circular polarization. Optik 200:163321. https://doi.org/10.1016/j.ijleo.2019.163321
20. Varshney G, Debnath S, Sharma AK (2020) Tunable circularly polarized graphene antenna for THz applications. Optik 223:165412. https://doi.org/10.1016/j.ijleo.2020.165412
21. Ezzulddin SK, Hasan SO, Ameen MM (2022) Microstrip patch antenna design, simulation and fabrication for 5G applications. Simul Model Pract Theory 116:102497. https://doi.org/10.1016/j.simpat.2022.102497
22. Nurrohman DT, Chiu N-F (2021) A review of graphene-based surface plasmon resonance and surface-enhanced raman scattering biosensors: current status and future prospects. Nanomaterials 11(1):216
23. Zhao T, Hu M, Zhong R, Gong S, Zhang C, Liu S (2017) Cherenkov terahertz radiation from graphene surface plasmon polaritons excited by an electron beam. Appl Phys Lett 110(23). https://doi.org/10.1063/1.4984961
24. Gusynin VP, Sharapov SG, Carbotte PG (2006) Magneto-optical conductivity in graphene. J Condens Matter Phys 19(2):026222. https://doi.org/10.1088/0953-8984/19/2/026222
25. Aloui R, Houaneb Z, Zairi H (2019) Substrate integrated waveguide circular antenna for terahertz application. Prog Electromagn Res C 96:229–242
26. Qin X, Chen J, Xie C, Xu N, Shi J (2016) A tunable THz dipole antenna based on graphene, in 2016 IEEE MTT-S International Microwave Workshop Series on Advanced Materials and Processes for RF and THz Applications (IMWS-AMP), IEEE 1–3
27. Abbasi QH, Alomainy A, Jornet JM, Han C, Chen Y (2018) Ieee access special section editorial: nano-antennas, nano-transceivers and nano-networks/communications. IEEE Access 6:8270–8272

28. Kumar MR (2019) A compact graphene based nano-antenna for communication in nano-network. J. IEICE 1(1):17–27

29. Correas-Serrano D, Gomez-Diaz JS, Perruisseau-Carrier J, Alvarez-Melcon A (2014) Graphene-based plasmonic tunable low-pass filters in the terahertz band. IEEE Trans Nanotechnol 13(6):1145–1153

30. Kushwaha RK, Karuppanan P, Malviya LD (2018) Design and analysis of novel microstrip patch antenna on photonic crystal in THz. Phys B Condens. 545:107–112. https://doi.org/10.1016/j.physb.2018.05.045

31. Shalini, M, Madhan MG (2019) Design and analysis of a dual-polarized graphene based microstrip patch antenna for terahertz applications. Optik 194:163050. https://doi.org/10.1016/j.ijleo.2019.163050

32. Li CH, Chiu TY (2017) 340-GHz Low-cost and high-gain on-chip higher order mode dielectric resonator antenna for THz applications. IEEE Trans Terahertz Sci 7(3):284–294. https://doi.org/10.1109/TTHZ.2017.2670234

33. Shamim SM, Uddin MS, Hasan MR, Samad M (2021) Design and implementation of miniaturized wideband microstrip patch antenna for high-speed terahertz applications. J Comput Electro 20(1):604–610. https://doi.org/10.1007/s10825-020-01587-2

34. Mondir A, Setti L, El Haffar R (2022) Design, analysis, and modeling using WCIP method of novel microstrip patch antenna for THz applications. Prog Electromagn Res C 125:67–82

35. Nickpay MR, Danaie M, Shahzadi A (2022) Wideband rectangular double-ring nanoribbon graphene-based antenna for terahertz communications. IETE J Res 68(3):1625–1634. https://doi.org/10.1080/03772063.2019.1661801

36. Kavitha S, Sairam KVSSSS, Singh A (2022) Graphene plasmonic nano-antenna for terahertz communication. SN Applied Sciences 4(4):114. https://doi.org/10.1007/s42452-022-04986-1

37. Khan MAK, Shaem TA, Alim MA (2019) Analysis of graphene based miniaturized terahertz patch antennas for single band and dual band operation. Optik 194:163012. https://doi.org/10.1016/j.ijleo.2019.163012

38. Deng X-D, Li Y, Liu C, Wu W, Xiong Y-Z (2015) 340 GHz on-chip 3-D antenna with 10 dBi gain and 80% radiation efficiency. IEEE Trans Terahertz Sci Technol 5(4):619–627

39. Khaleel SA, Hamad EKI, Saleh MB (2022) High-performance tri-band graphene plasmonic microstrip patch antenna using super-strate double-face metamaterial for THz communications. J Electr Eng 73(4):226–236. https://doi.org/10.2478/jee-2022-0031